Available online at www.sciencedirect.com

ScienceDirect

Procedia Structural Integrity 7 (2017) 141–148

Structural Integrity Procedia

www.elsevier.com/locate/procedia

3rd International Symposium on Fatigue Design and Material Defects, FDMD 2017, 19-22 September 2017, Lecco, Italy

Damage development and damage tolerance of structures manufactured by selective laser melting – a review

U. Zerbst * and K. Hilgenberg

Bundesanstalt für Materialforschung und -prüfung (BAM), Unter den Eichen 87, D-12205 Berlin, Germany

Abstract

The additive manufacturing technology of Selective Laser Melting (SLM) experiences a rapid development within an increasing marked of quite different application fields. The properties of SLM materials and structures are influenced by a number of technological parameters such as the metal powder (particle size, homogeneity, cleanliness), the laser tool (power, beam diameter, pulse lengths), the scanning operation (speed, sequence and orientation of melting paths), parameters of the over-all equipment (design and preheating of the base plate, currents and turbulence in the protective gas atmosphere) and, last not least, the hatching strategy including the build-up direction of the structure with respect to the loading direction of the component.

For the perspective use of SLM structures as load carrying, safety-relevant components the knowledge of their mechanical properties is necessary. It is essential to understand these in the context of the manufacturing-related features and at the background of the basic characteristics of metallic materials: crystal lattice, microstructure and material defects. The paper provides an overview on factors which affect the mechanical parameters stiffness, strength, ductility, toughness, fatigue crack propagation and fatigue strength in the context of selective laser melting.

Peer-review under responsibility of the Scientific Committee of the 3rd International Symposium on Fatigue Design and Material Defects.

Keywords: Fatigue strength; fracture mechanics; initial crack size; short crack propagation; multiple crack propagation

Introduction

Fig. 1 (a) gives an overview on the factors that influence the principal mechanical properties of metallic materials (stiffness, strength, ductility, toughness, fatigue crack propagation and fatigue strength). These properties are affected by the materials basic characteristics (crystal lattice, microstructure and material defects) in quite different ways. In the following sections a brief overview is provided on the potential relationships with special emphasis to structures manufactured by Selective Laser Melting (SLM). Because of its paramount importance, this shall be preceded by the definition of the build-up direction with respect to the applied

* Corresponding author. Tel.: +49 (0) 30 8104 1531; fax: +49 (0) 30 8104 1537.
E-mail address: uwe.zerbst@bam.de

Peer-review under responsibility of the Scientific Committee of the 3rd International Symposium on Fatigue Design and Material Defects.
10.1016/j.prostr.2017.11.071

loading direction in different test configurations (Fig. 1b). For the fracture mechanics specimens, the nomenclature of ISO 12135 (2002) is used.

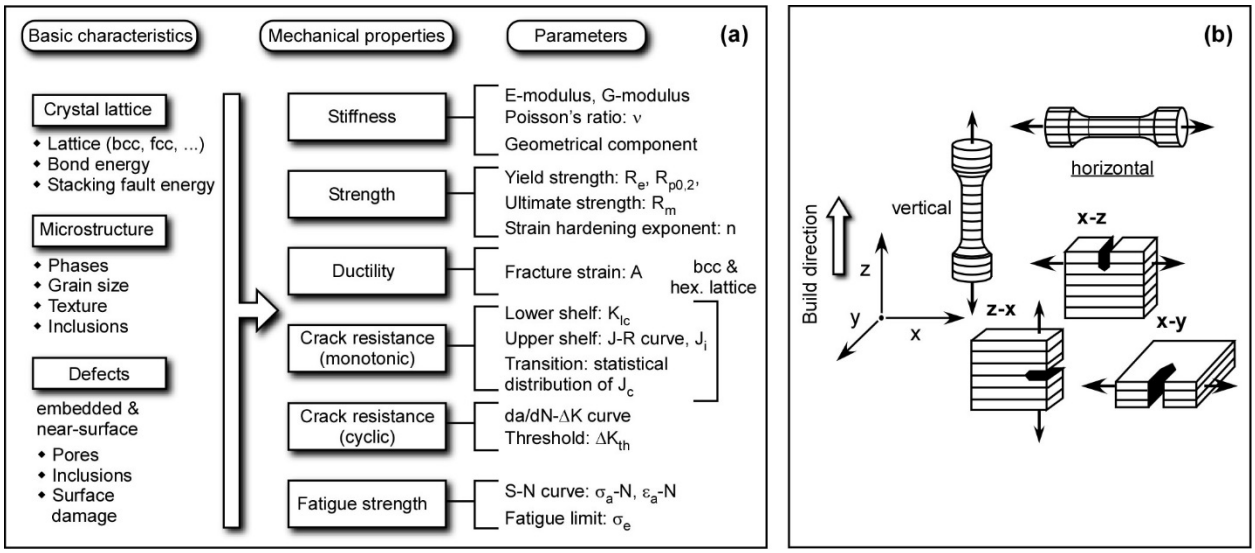

Fig. 1 (a) Relations between the basic characteristics, the basic mechanical properties and the mechanical parameters describing the latter in metallic materials; (b) Nomenclature for the build-up orientation with respect to the applied loading direction in SLM structures.

Stiffness

The stiffness, which is important with respect to the elastic form stability of components as well as for the avoidance of local stress concentrations due to stiffness discontinuities in compounds, e.g., between implants and bones, is usually characterized by the modulus of elasticity which is a function of the crystal properties, particularly the metal bounding and which can be influenced by alloying with high-melting elements (Rösler et al., 2006). Note, however, that stiffness is not only a materials property. Not least SLM provides unique possibilities for influencing this property by "tailoring" the internal structure of components, e.g., by the build-up of controlled porous and net-like patterns, e.g. Rotta et al. (2015). It should, however, be noted that porosity, beside the stiffness, also affects other properties such as the strength and the fatigue strength, usually in a negative way with respect to component performance, e.g., Ahmadi et al. (2016).

Strength and ductility

Besides the lattice type, which determines the number of active slip systems, the strength of polycrystalline materials is controlled by strengthening mechanisms such as grain boundary strengthening (of Hall-Petch materials with low stacking fault energy), solid solution strengthening, precipitation hardening or strain hardening. Fig. 2 shows two examples for the influence of SLM on the stress-strain behavior of austenitic steels (Cartlon et al., 2016; Meier & Haberland, 2006). Compared to the reference mate-rials manufactured by conventional technology both, an increased strength and a reduced ductility (in terms of the fracture strain) can be stated. Note that this is a quite common pattern also for other materials. Reasons are the steep temperature gradients, rapid solidifycation and fast cooling of the very small material volume of a SLM "welding layer" which cause martensitic transforma-tion (in titanium alloys (e.g., Vrancken et al., 2012), dendritic fine columnar microstructures in austentitic steel (e.g., Carlton et al, 2016), etc. As the consequence, subsequent heat treatment of the as-built components becomes necessary in many cases. An example for this is shown in Fig. 2 (b). Besides the metastable microstructure, other features such as porosity as a material defect affect the stress strain properties of SLM structures. Note that porosity is a problem of SLM which it shares with technologies such as sintering, casting and (partially) welding, however, enhanced by texture formation due to the build-up process. Pores can be the result of unmelted powder, the balling effect or gas entrapment. Which mechanism dominates and how pronounced the effect is, is affected by the technological parameters, most of all the laser power and scanning speed (Kasperovich et al., 2016). Ibbett et al. (2105) demonstrate in a numerical simulation of the crack behavior of Nylon-12 that the location, the size and the number of unmelted particles can have a significant effect not only on crack initiation but also on crack paths. It is not hard to imagine that any texturizing of porosity, e.g., following the build-up pattern might be dramatic for properties such as ductility and fatigue crack propagation and, in combination with these, fracture toughness and the fatigue strength. The disadvantageous effect of porosity on the ductility is illustrated in Fig. 2 (a) and (b). Fig. 2 (c) shows the effects of the build-up direction and layer thickness. Note that

they are particularly problematic for vertical build-up where the layer interfaces from the subsequent SLM steps are oriented perpendicular to the loading direction. An indirect evidence of the influence of porosity on the ductility is provided by the beneficial effects of hot isostatic pressing (HIP), see, e.g., Siddique et al. (2015b) and Tomus et al. (2016). The effect of HIP treatment is a reduction of inner porosity of materials.

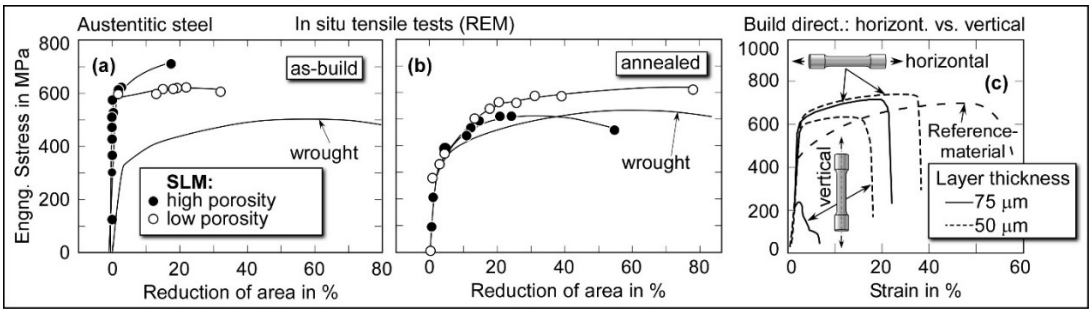

Fig. 2: Engineering stress-strain curves of 316L steels manufactured by SLM. (a) and (b) Effects of porosity and annealing; according to Carlton et al., 2016); (c) Effect of the build-up direction with respect to the loading direction and of the layer thickness; according to Meier & Haberland, 2008).

A specific problem with respect to the ductility of SLM structures is reproducibility. Salzbrenner et al. (2017), testing a number of 120 small scale tensile specimens (cross section 1 x 1 mm^2) of SLM manufactured stainless martensitc steel, found the lower bound of the scatter band shifted to smaller ductility values when compared to the trend of the Weibull distribution fitted to the complete data set. From a statistical point of view, this points to different sampling, i.e., different material states erroneously assigned to one distribution. The authors suspect as potential causes, besides deviations from the target microstructure, internal lack-of-fusion porosity and surface roughness (although the latter should not be relevant for tensile test data which require smooth specimens).

Fracture toughness

Only few fracture toughness data sets are available of SLM manufactured materials in the literature. An example for Ti6Al4V is provided in Table 1 (Cain et al., 2015). As can be seen, the as-built properties referring to the z-x direction are the poorest. Note that this direction refers to the SLM layers oriented normally to the loading direction. One could suspect material weakening at this planes, e.g., due to microstructure anisotropy or a texturized defect pattern which cause local stress concentrations as the reason. Whatever the cause might be, a disadvantageous effect of specimens with the building direction being the same as the loading direction (i.e. the interfaces between the layers being perpendicular to it) is also stated by Edwards et al. (2015). Note that the discussion of the toughness topic of SLM structures is a bit hampered by the circumstance that quite a few published data use outdated fracture mechanics concepts such as the determination of the CTOD from the maximum load in the test record.

Table 1: Fracture toughness of SLM manufactured Ti6Al4V in the as-built, stress relieved and heat treated state; according to Cain et al., (2016).

Fracture toughness K_{Ic} in MPa $m^{1/2}$			
Specimen orientation with respect to build-up direction	as-built	stress relief treatment (650ºC, 2 hours)	annealed (890ºC, 2 hours)
x-y	28 ± 2	28 ± 2	41 ± 2
x-z	23 ± 1	30 ± 1	49 ± 2
z-x	16 ± 1	31 ± 2	49 ± 1

With respect to a general scheme of factors influencing the fracture toughness, all three features of the basic material characteristics of Fig. 1, crystal lattice, microstructure and material defects, play a role. E.g., only materials with a limited number of active slip systems, i.e. bcc or hexagonal ones will show a distinct ductile-to brittle transition, and its manifestation will depend on the materials ductility which in turn is influenced by parameters such as the temperature or loading rate.

(i) The common concept of toughness at the lower shelf follows a multi-barriers model (Chen & Cao, 2015, Pineau et al., 2016) consisting of the subsequent steps of microcrack nucleation usually at brittle inclusions, the growth of the crack through the particle or along the particle-matrix boundary, its transition into an adjacent grain and, from there, through the cross section of the component. The possibility of crack arrest at a grain boundary points to the potential effect of the grain size on the lower shelf toughness. There might be, however, a situation of competition between different microstructural items such as, e.g., ferrite grain boundaries and carbide particles in ferritic steel. Which of these will finally control the fracture process depends on the ductility of

the material, i.e. in an indirect way on the temperature and loading rate. The parameter describing the toughness in the lower shelf is the plane-strain fracture toughness K_{Ic}.

(ii) At the upper shelf, the failure process consists in three steps (Pineau et al., 2016): the nucleation of voids in the plastic deformed material preferably at inclusions, the growth of this voids and its final coalescence by overcoming the remaining material bridges. Usually most of the dissipated energy is spent for the plastification of the bulk material and only a minor part is con-sumed at the crack tip (Brocks et al., 2003). The J integral as the preferred parameter for upper shelf toughness accumulates both portions because of which it might be expected to be influenced by the same parameters as the ductility of the material.

(iii) The ductile-to-brittle transition combines elements of both, the lower and the upper shelf. Defects and defect clusters which immediately had triggered the failure at the slower shelf are "defused", i.e. the micro-notches are rounded off due to the higher ductility of the material. A limited number of defects, however, remains critical when the peak stress in the ligament is shifted to their positions. Note that the stress ahead of the crack tip reaches a maximum at a distance of 1.6 to 2.4 times the crack tip displacement CTOD (depending on the strain hardening capacity of the material, Chen & Cao, 2015) and that it is shifted into the ligament with load increase and crack extension (Heerens et al., 1993). The limited number of critical defects (which might be inclusions, inclusion clusters, brittle zones of microstructure, etc.) is responsible for the significant scatter band, which is characteristic for the fracture toughness in the ductile-to-brittle transition range. When the critical defect site is close to the crack front, the stress peak has to be shifted into the ligament by a small amount only, but when it is far, this amount will be much larger. This difference is mirrored in the different energy supplied and thus in the different fracture resistance from specimen to specimen. The latter is obtained as the J integral at the failure load but then processed statistically with a validity criterion applied to the lower shelf of the distribution. In cases of material inhomogeneity such as weldments or (potentially) SLM configurations, the same problem is expected as discussed above in the context of the reproducibility of ductility. The mixture of different samples, i.e., microstructures may cause problems in statistical treatment with the result of an overestimation of the lower bound toughness – but this, at present, is an academic problem of SLM because of the lack of experimental data.

Fatigue crack propagation

Fatigue propagation is commonly described by the da/dN-ΔK curve, which consists of the three branches of (i) the threshold region, (ii) the Paris region (where da/dN-ΔK gives a straight line in double-logarithmic scaling) and (iii) the transition to the final fracture region. No exhaustive discussion is possible here because of the limited space. A phenomenon that plays a major role in fatigue crack propagation is so-called crack closure. A crack propagates only when it is open. E.g., for a load ratio of $R = \sigma_{min}/\sigma_{max}$ or $K_{min}/K_{max} = -1$, half the loading cycle is in compression. As the consequence, the effective part of the cyclic K factor ΔK ($= K_{max} - K_{min}$), ΔK_{eff} is no more than ½ ΔK. In reality, it is even smaller due to the crack closure phenomenon. Several me-chanisms are responsible for this with the three most important ones being the plasticity-, the roughness- and the oxide-debris-induced ones (Suresh, 2003). When loaded, a plastic zone forms ahead of the crack tip, which remains at the crack wake when the crack propagates. The consequence of the "frozen" plastic deformation is some geometrical misfit of the corresponding crack faces, and the crack closes at a load higher than the zero transition of the stress. The phenomenon is designated by plasticity-induced crack closure. Roughness-induced crack closure is caused by a geometrical misfit of the crack faces due to local mixed mode effects enhanced by crack deviation from its growth area or crack branching. The oxide-debris-induced effect is caused by the oxidation of the crack faces. At low R ratios these are "furbished" with the result of addition oxidation and a thickness in-crease of the oxide debris layer. Whilst the plasticity-induced effect plays a role over the whole da/dN-ΔK diagram, the toughness- and oxide-debris-induced ones are most important in the threshold region. The crack closure phenomenon is one of two mechanisms responsible for the R ratio (or mean stress) dependency of the da/dN-ΔK curve. Whilst there is no closure effect at high R ratios, where the crack is fully open, it increases with decreasing R ratio. The second R effect on da/dN-ΔK consists in monotonic failure mechanisms at the upper load, σ_{max} or K_{max}, in the loading cycle. This is typical in the transition to the final fracture region, where limited cleavage or ductile failure events are interspersed with the effect of speeding up the crack propagation rate causing a steeper da/dN-ΔK curve compared to the Paris range.

These preliminary remarks were necessary for the interpretation of the information provided in Fig. 3. Fig. 3 (a) shows Paris range da/dN-ΔK curves of sinter steel batches of different density (Fleck & Smith, 1981). As can be seen, the lower density corresponds with a steeper da/dN-ΔK curve. An explanation is that the higher pore volume causes an increase in the crack propagation rate in that the crack – by an alternative propagation mechanism – "jumps" through the cavities. An indirect but similar result is reported by Feng et al. (2013) on Ti6Al4V cast alloy in the as-cast state and after treatment by hot isostatic pressing (HIP). As mentioned, the effect of HIP is the densification of the material, i.e. a reduction of its porosity. Following the same explanation as above, HIP should yield a less steep da/dN-ΔK curve, and that is exactly what the authors observed. The cited results were obtained on sinter and cast alloys but similar effects are to be expected for other porous materials as well, and SLM manufactured structures definitely belong to this group. Fig. 3 (b) provides a comparison of da/dN-ΔK curves of SLM and conventionally manufactured Inconel 718 (Konečná et al., 2016). Whilst the curves run into a common scatter band for higher ΔK, there is a significant difference in the threshold region in that the crack of the SLM alloy growths much faster such as if the crack were loaded by a higher R ratio or, in other words, it would not experience any crack closure effect. The authors discuss their result with respect to three observations.

(i) First, their SLM alloy contains a very low content of boron and this is known to be disadvantageous with respect to the crack propagation threshold. (ii) Second, it is characterized by a much finer grain compared to, at least, one of the conventional alloys in the figure. It is common knowledge that a finer grain shifts the threshold to lower values whilst the fatigue strength is increased (Pleghov et al., 2011). An explanation is that the finer grain usually corresponds with smoother crack faces and that this, in turn, reduces the roughness-induced crack closure effect. As the consequence, ΔK_{eff} becomes larger. (iii) As the third effect the authors suspect tensile residual stresses at the crack tip which also keep the crack open. Since residual stresses act like mean stresses, both, K_{max} and K_{min} are increased and so is the R ratio with the effect that any crack closure effect is reduced. That substantial tensile residual stresses can be build-up in SLM structures is illustrated in Fig. 3 (c), Edwards & Ramulu (2014). Residual stresses in SLM structures is a field of its own. Although a lot of work is spent in that context, no detailed discussion will be provided here (for a limited overview see the citations in Zerbst & Hilgenberg, 2017). Note that a result such as that in Fig. 3 (c) cannot be generalized because the residual stress pattern depends on a wide range of factors such as the hatching strategy, pre-heating of the base plate, the overall geometry of the structure etc.

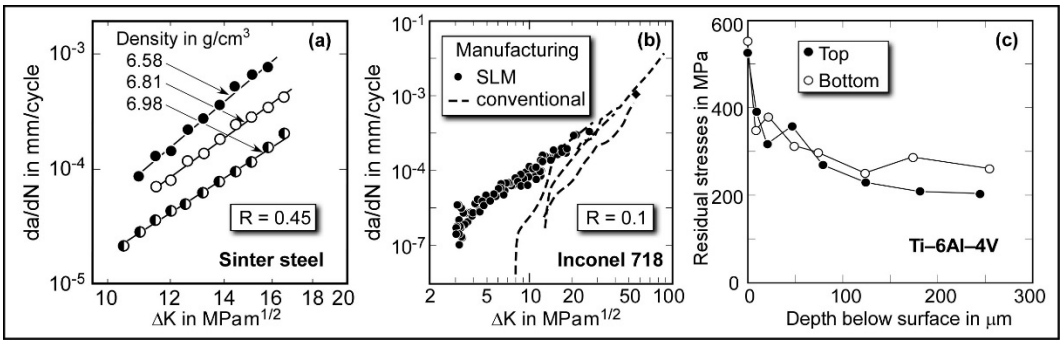

Fig. 3: Effects on the da/dN-ΔK characteristics. (a) Effect of the density on the slope of the Paris range da/dN-ΔK curve of different batches of a sinter steel, according to Fleck & Smith (1981); (b) Differences in the threshold range da/dN-ΔK characteristics of SLM and conventionally manufactured Inconel 718, according to 718 Konečná et al. (2016); (c) In thickness residual stress profiles of SLM manufactured Ti6Al4V, according to Edwards & Ramulu (2014).

Fatigue strength

The overall lifetime of a structure containing a fatigue crack consists of different stages. This is illustrated in Fig. 4. The crack nucleation due to the accumulation of plastic strain is followed by the stage of short crack propagation and this will be followed by the stage of long crack propagation until failure. Since the nucleation stage (in the narrower sense) is rather short in many cases or even disappears in the presence of crack-like initial defects in the material (Polak, 2003) the major part of the lifetime is usually spent at the short crack stage. In that context, two explana-tions are due. First, besides the definitions of the crack growth stages used in this paper an "engineering" definition is common which subsumes crack nucleation and short crack propagation up to a crack size visible per eye as the initiation phase. Second, the short crack stage such as used in the present paper has to be subdivided in turn. A first stage of microstructural short cracks with a size in the order of microstructural units such as the grain size is followed by a stage of mechanically/physically short cracks which beyond a certain size become large cracks. No detailed discussion of these issues shall be provided here, see, however, Zerbst et al. (2007).

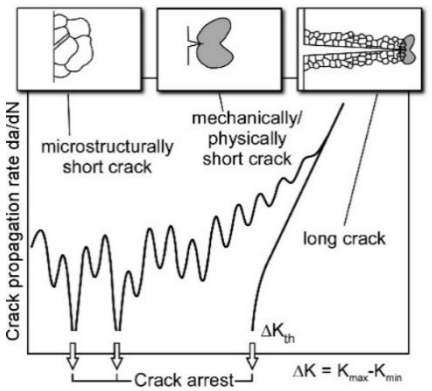

Fig. 4: Stages of fatigue crack propagation.

What is important in the context of the fatigue strength is that the endurance limit per definition is a matter of crack arrest. (i) Microstructurally short cracks arrest at microstructurally features, mainly grain boundaries when the grain ahead of the crack tip is characterized by a different crystallographic orientation. (ii) Physically short cracks arrest due to the gradual build-up of the crack closure effects which require some crack length which is not given at the beginning of crack growth. (iii) Long cracks, the definition of which is that the closure mechanisms are stabilized, i.e., crack length independent, arrest when the crack driving force is below the long crack threshold ΔK_{th}. (iv) Finally, a frequent cause of crack arrest is that a crack grows in a decreasing stress field, usually

in a notch. Note that the endurance limit disappears when mechanisms exist which overcome the barriers, e.g., time dependent corrosion mechanisms.

Keeping this in mind, the fatigue strength of metallic materials is affected by material defects which act as crack initiation sites usually at the surface, and by defects at the crack propagation path in the inner. Typical defects of SLM structures are pores, surface roughness, oxide inclusions (in some cases) and, sometimes in conjunction with these, microcracks.

(a) Pores

As mentioned above, porosity in SLM can be the consequence of locally unmelted powder or gas entrapment due to turbulent currents in the protective gas atmosphere at the surface of the metal or overheating of the molten pool. A third possibility is shrink cavities. That pores or pore clusters act as crack initiation sites is, e.g., reported by Brandl et al. (2012), Chan et al. (2012) and Edwards & Ramulu (2014). Whilst crack initiation at the surface in conventional materials usually widely controls the fatigue life, there seems to be a more pronounced effect of crack propagation across the section in SLM structures. An indirect indication for this is reported by Zhao et al. (2016), who found a substantial improvement of a Ti6Al4V S-N curve after the specimens were treated by hot isostatic pressing (HIP), which has an effect only on the inner part of the structure, Fig. 5 (a). A similar effect was found by Günther et al. (2017) for very high cycle fatigue (VHCF, more than 10^7 loading cycles) also of Ti6Al4V.

(b) Surface roughness

Besides pores and micro-cavities, adhesion of not completely melted powder particles contribute to surface roughness such that the latter is a genuine property of SLM structures. Its magnitude widely depends on technological parameters such as scanning speed and the laser power, but also the orientation of the surface with respect to the build-up direction plays a role (Meier & Haberland, 2008). The effect of surface roughness on the fatigue strength is illustrated in Fig 5 (b) where the S-N curves of as-build and surface milled specimens of Ti6Al4V are compared (Greitemeier et al., 2015). As can be seen, surface smoothing significantly improves the fatigue strength. The dependency of the S-N curve on the build-up direction is illustrated by the example in Fig. 5 (c) on an aluminium alloy (Brandl et al., 2012). A similar effect is reported by Kajima et al (2016) for a Co-Cr-Mo alloy.

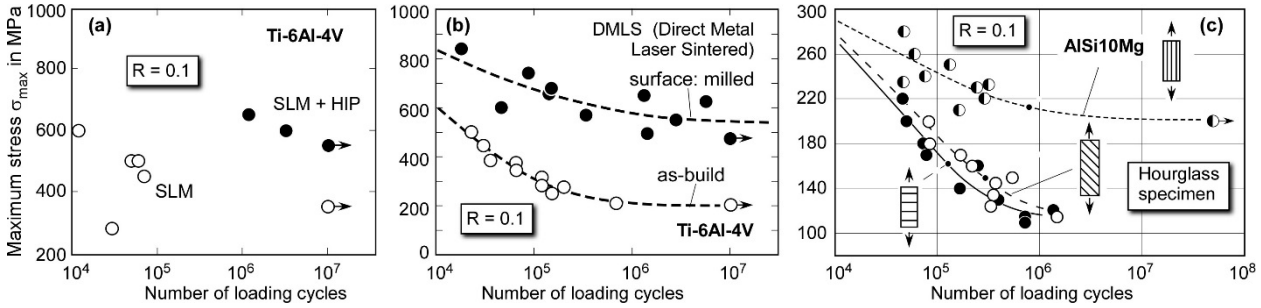

Fig. 5: S-N curves of (a) Ti6Al4V in the as-build and HIPed state, according to Zhao et al. (2016); (b) Ti6Al4V in the as-build and surface milled state, according to Greitemeier et al. (2015); (c) AlSi10MG for different build-up directions with respect to the loading direction, according to Brandl et al. (2012).

(c) Oxide inclusion

Oxide inclusion is quite common in aluminium alloys (Olakanmi et al., 2015), although it is not restricted to this material class (Vranken et al, 2013). The mechanism by which oxide films built-up between the laser hatches of the SLM layers and how these are incorporated in the bulk material where they can act as internal stress concentrators is illustrated in Fig. 6. That relatively large oxides can also form by the oxidation of vaporized metal is reported by Tang and Pistorius (2017).

(d) Microcracks

Comparable to the welding process, solidification cracks can form in SLM manufactures structures (Olakanmi et al., 2015), e.g., at oxide inclusions such as described above or as the consequence of shrinkage (residual) stresses during cooling (Vrancken et al., 2013). Cloots et al. (2016) point to an interrelation between cracks and pores in that the microcrack density in a nickel-based superalloy is reduced with increasing porosity.

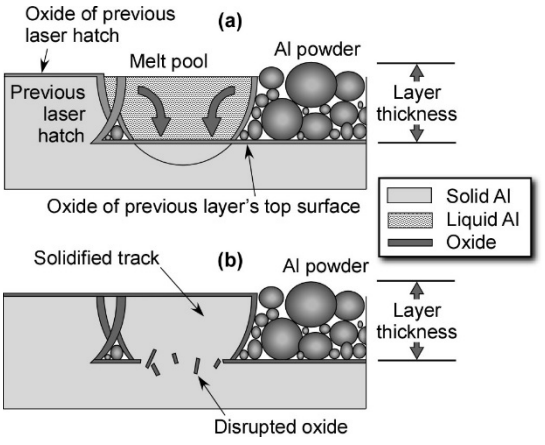

Fig. 6: Penetration of oxide layers into the welding of an aluminium alloy; according Olakanmi et al. (2015).

(e) Residual stresses

The effect of residual stresses on fatigue crack propagation has already been briefly addressed. That residual stresses have also an effect on the fatigue strength is well known and does not need a separate discussion. The example of Fig. 3 (c) shows that they can be of significant magnitude at the surface in the as-build state of SLM structures. Frequently, high tensile residual stresses are found in the last surface layer (e.g., Shiomi et al., 2004). The most important measure for reducing the residual stresses during manufacturing is base plate heating, methods for reducing them subsequent to the manufacturing process are stress relief head treatment and laser rescanning of the surface (Shiomi et al., 2004, Kruth et al., 2012). In principle, any measure that reduces the high thermogradient should be of benefit (and that not only with respect to the residual stresses). That there is an influence of the build-up direction on residual stress formation is shown by Vrancken et al. (2014), who also found it to be relevant with respect to the effect of stress relief. Only for x-z and z-x build-up directions of their fracture mechanics specimens made of Ti6Al4V a beneficial effect was observed whereas for the x-y direction no to detrimental effects were stated. The observation that the biggest benefit for the crack propagation resistance is achieved when the build-up and loading directions are identical, i.e., the layer interfaces are oriented perpendicular to the loading direction, is also confirmed by Cain et al. (2015). No further effect of heat treatment on the residual stresses was found by Siddique et al. (2015a) on AlSi12 when base plate heating occurred during manufacturing

References

Ahmadi, A., Mirzaeifar, R., Moghaddam, N.S., Turabi, A.S., Karaca, H.E and Elahinia, M. (2016): Effect of manufacturing parameters on mechanical properties of 316L stainless steel parts fabricated by selective laser melting: A computational framework. Mat. Design 122, 328-338.

Brandl, E., Heckenberger, U., Holzinger, V. und Buchbinder, D. (2012): Additive manufactured AlSi10Mg samples using Selective Laser Melting (SLM): Microstructure, high cycle fatigue, and fracture behavior. Mat. Design 34, S. 159-169.

Brocks, W., Cornec, A. and Scheider, I. (2003): Computational aspects of nonlinear fracture mechanics. In: Milne, I., Ritchie, R.O. and Karihaloo, B. (eds.): Comprehensive Structural Integrity (CSI), Elsevier, Amsterdam et al., Vol. 3, 3.03, 129-209.

Cain, V., Thijs, L., van Humbeeck, J. and Knutsen, R. (2015): Crack propagation and fracture toughness of Ti6Al4V alloy produced by selective laser melting. Add. Manu. 5, 68-76.

Carlton, H.D., Haboub, A., Gallegos, G.F., Parkinson, D.Y. and McDowell, A. (2016): Damage evolution and failure mechanism in additively manufactured strainless steel. Mat. Sci. Engng. A 651, 406-414.

Chan, K.S., Koike, M., Mason, R.L. und Okabe, T. (2012): Fatigue life of titanium alloys fabrikated by additive layer manufacturing techniques for dental implants. Metallurgical and Mat. Trans 44A, S. 1010-1022.

Chen, J.H. and Cao, R. (2015): Micromechanisms of cleavage of metals. A comprehendsive microphysical model for cleavage cracking in metals. Elsevier, Amsterdam et al.

Cloots, M., Uggowitzer, P.J. und Wegener, K. (2016): Investigations on the microstructure and crack formation of IN738LC samples processed by selective laser melting using Gaussian and doughnut profiles. Materials & Design 89, 770-784.

Edwards, P. und Ramulu, M. (2014): Fatigue performance evaluation of laser-melted Ti-6Al-4V. Mat. Sci. & Engng. A 598, S. 327-337.

Edwards, P. and Ramulu, M. (2015): Effect of build direction on the fracture toughness and fatigue crack growth in selective laser melted Ti-6Al-4V. Fatigue Fracture Engng. Mat. Struct. 38, 1228-1236.

Feng, X., Wang, A., Ma, Y., Wu, X., Lei, J., Cui, Y. und Yang, R. (2013): Influence of microstructure on fatigue crack propagation and fracture. 13th International Conference on Fracture (ICF 13), Beijing, China.

Fleck, N.A. and Smith, R.A. (1981): Effect of density on tensile strength, fracture toughness and fatigue crack propagation behavior of sintered steel. Powder Met., 3, S. 121-125.

Greitemeier, D., Holzinger, V., Dalle Donne, C., Eufinger, J. und Melz, T. (2015): Fatigue prediction of additive manufactured Ti-6Al-4V for aerospace: Effect of defects, surface rough-ness. 28. ICAF Symp. Helsinki.

Günther, J., Krewerth, D., Lippmann, T., Leuders, S., Tröster, T., Weidner, A., Biermann, H. and Niendorf, T. (2017): Fatigue life of additively manufactured Ti–6Al–4V in the very high cycle fatigue regime. Int. J. Fatigue 94, 236-245.

Heerens, J., Zerbst, U. and Schwalbe, K.-H. (1993): Strategy for characterizing fracture toughness in the ductile to brittle transition regime. Fatigue Fracture Engng. Mat. Struct. 16, 1213-1230.

Ibbett, J., Tafazzolimoghaddam, B., Delgadillo, H. and Curiel-Sosa, J.L. (2015): What triggers a microcrack in printed engineering parts produced by selective laser sintering on the first place? Mat. & Design 88, S. 588-597.

ISO 12135 (2002): Metallic materials – Unified method of test for the determination of quasistatic fracture toughness. International Organization for Standardization, Geneva.

Kajima, Y., Takaichi, A., Nakamoto, T., Kimura, T., Yogo, Y., Ashida, M., Doi, H., Nomura, N., Takahashi, H., Hanawa, T. and Wakabayashi, N. (2016): Fatigue strength of Co-Cr-Mo alloy claps prepared by selective laser melting. J. Mech. Behavior Biomedical Mat. 59, 446-458.

Kasperovich, G., Haubrich, J., Gussone, J., Requena, G. (2016): Correlation between porosity and processing parameters in TiAl6V4 produced by selective laser melting. Mater. Des. 105, 160–170.

Konečná, R., Kunz, L., Nicoletto, G. und Bača, A. (2016): Long fatigue crack growth in Inconel 718 produced by selective laser melting. Int. J. Fatigue 92, 499-506.

Kruth, J.-P., Deckers, J. Yasa, E. and Wauthle, R. (2012): Assessing and comparing influencing factors of residual stresses in selective laser melting using a novel analysis method. Proc. IMech E, Part B: J Engng. Manufacture 226, 980-991

Meier, H. and Haberland, C. (2008): Experimental studies on selective laser melting of metallic parts. Mat.-wiss. & Werkstofftechn. 39, S. 665-670.

Olakanmi, E.O., Cochrane, R.F. und Dalgarno, K.W. (2015): A review on selective laser sintering/melting (SLS/SLM) of aluminium alloy powders: Processing, microstructure, and properties. Progress in Mat Sci. 74, 401-477.

Pineau, A., Benzerga, A.A. an d Pardoen, T. (2016): Failure of metals I: brittle and ductile fracture. Acta Mat. 107, 424-438.

Plekhov, O., Paggi, M., Naimark, O. und Carpinteri, A. (2011): A dimensional analysis interpretation to grain size and loading frequency dependencies of the Paris and Wöhler curves. Int. J. Fatigue 33, 477-483.

Polak, J. (2003): Cyclic deformation, crack initiation, and low-cycle fatigue. In: Ritchie, R.O. and Murakami, Y. (Eds.): Comprehensive Structural Integrity; Volume 4: Cyclic loading and Fracture; Elsevier, 1-39.

Rösler, J., Harders, H. and Bäker, M. (2006): Mechanisches Verhalten der Werkstoffe. Teubner. Wiesbaden, 2nd. ed.

Rotta, G., Seramak, T. and Zasinska, K. (2015): Estimation of the Young's modul of the porous titanium alloy with the use of FEM package. Advances in Mat Sci. 15, 29-37

Shiomi, M., Osakada, K., Nakamura, K, Yamashita, T. und Abe, F. (2004): Residual stress within metallic model made by selective laser melting process. CIRP Annals – Manufact. Techn. 53, S. 195-198.

Siddique, S.,Imran, M., Wycisk, E., Emmelmann, C. and Walther, F. (2015a): Influence of process-induced microstructure and imperfections on mechanical properties of AlSi12 processed by selective laser melting. J. Mat. Processing Techn. 221, 205-213.

Siddique, S.,Imran, M., Rauer, M., Kaloudis, M., Wycisk, E., Emmelmann, C. and Walther, F. (2015b): Computed tomography for characterization of fatigue performance of selective laser melted parts. Mat. Design 83, 661-669.

Suresh, S., 2003. Fatigue of materials. Cambridge: Cambridge University Press, 2nd ed.

Tang, M. and Pistorius, P.C. (2017): Oxides, porosity and fatigue performance of AlSi10Mg parts produced by selective laser melting. Int. J. Fatigue 94, 192-201.

Tomus, D., Tian, Y., Rometsch, P.A., Heilmaier, M. and Wu, X. (2016): Influence of post heat treatments on anisotropy of mechanical behavior and microstructure of Hastelloy-X parts produced by selective laser melting. Mat. Sci. Engng. A 667, 42–53.

Vrancken, B., Cain, V., Knutsen, R. und van Humbeeck, J. (2014): Residual stress via the contour method in compact tension specimens produced via selective laser melting. Scripta Mat. 87, S. 29-32.

Vrancken, B., Thijs, L., Kruth, J.-P. and van Humbeck, J. (2012): Heat treatment of Ti6Al4V produced by selective laser melting: mictrostructure and mechanical properties. J. Alloys Compounds 541, 177-185.

Vrancken, B., Wauthle, R., Kruth, J.-P. und Humbeek, J. (2013): Study of the influence of material properties on residual stress in selective laser melting. Proc. Solid Freedom Fabrication Symp., Austin, S. 1-15.

Zerbst, U. and Hilgenberg, K. (2017): Schadensentwicklung und Schadenstoleranz von SLM-gefertigten Strukturen. In: Richard, H. A., Schramm, B. and Zipsner, T.: Additive Fertigung von Bauteilen und Strukturen. Springer Vieweg, Wiesbaden 2017.

Zerbst, U., Madia, M., Vormwald, M. and Beier, H.Th. (2017): Fatigue strength and fracture mechanics – a general perspective. Subm. to Engng. Fracture Mech.

Zhao, X., Li, S., Zhang, M. Liu, Y., Sercombe, T.B., Wang, S., Hao, Y., Yang, R. und Murr, L.E. (2016): Comparison of the microstructures and mechanical properties of Ti–6Al–4V fabricated by selective laser melting and electron beam melting. Mat. & Design 95, 21-31.